Electronic Supplementary Material (ESI) for Inorganic Chemistry Frontiers.

Support information

Compatible and high-efficiency quasi-solid-state integrated photo-capacitor based on synergistic of PEDOT/RGO electrode and electrolyte to improve carrier migration

Yuanduo Qu, Siqi Liao, Liangyi Wu, Junkai Wang, Lianfeng Duan*, Xia He, Fushen Lu*

Department of Chemistry and Key Laboratory for Preparation and Application of Ordered Structural Materials of Guangdong Province, Shantou University, Shantou 515063, China

*Corresponding authors

E-mail address: lfduan@stu.edu.cn (L. Duan), fslu@stu.edu.cn (F. Lu)

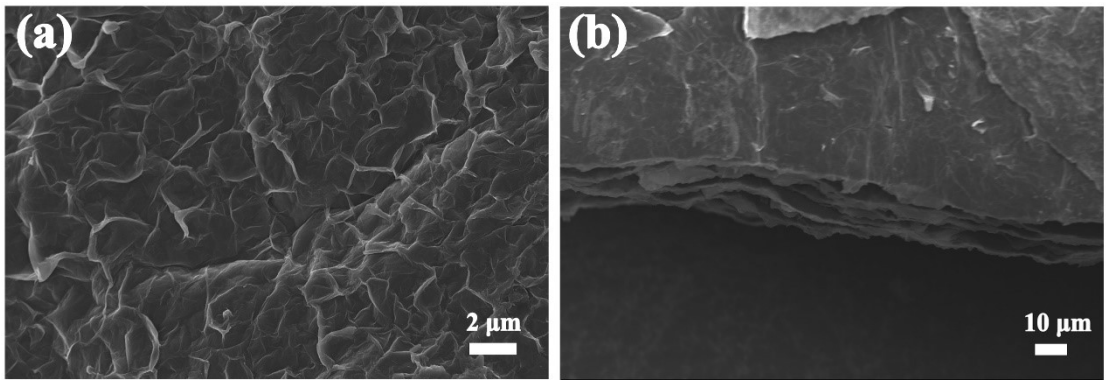

Figure S1 (a) The top-view and (b) cross-view SEM images of RGO film.

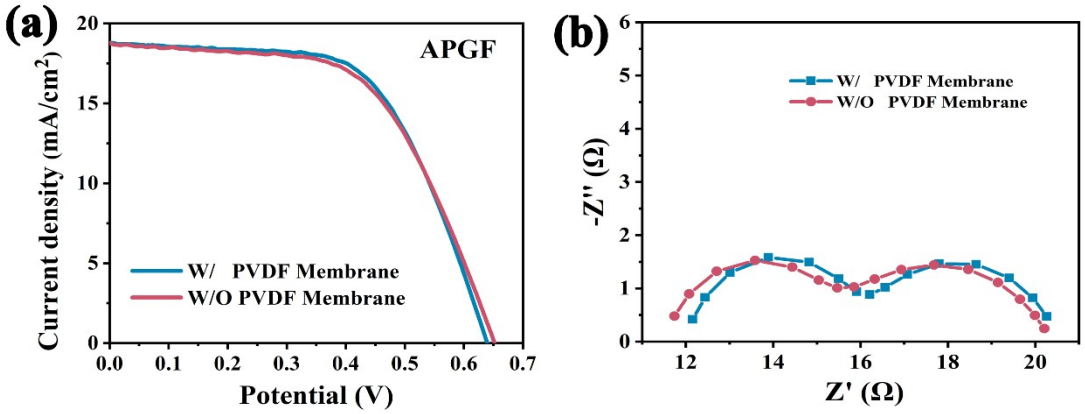

Figure S2 (a) The J-V curves and (b) EIS spectra of DSSCs with or without electro-spun PVDF nanofiber membrane.

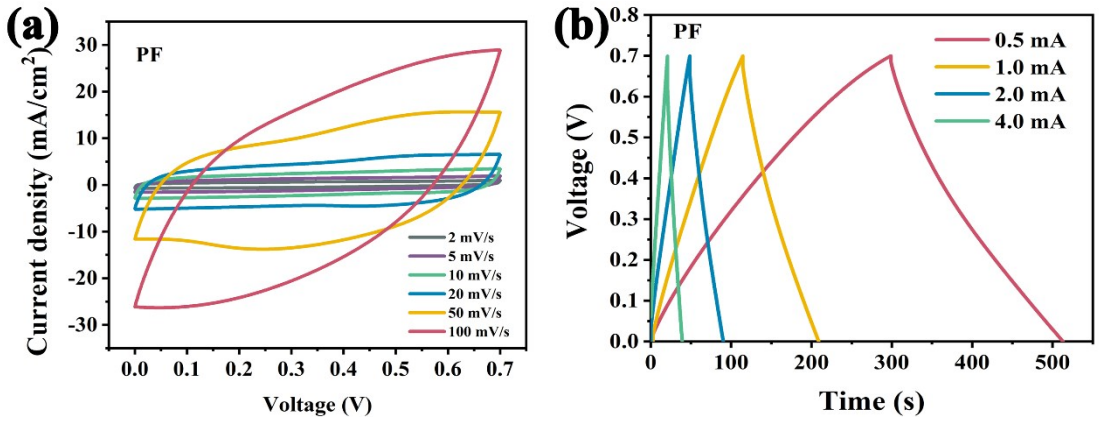

Figure S3 (a) The CV curves of all-solid-state supercapacitors based on $BMIMBF_4$ gel electrolyte at various scan rates and (b) the GCD curves at different discharge currents with PF as electrode.

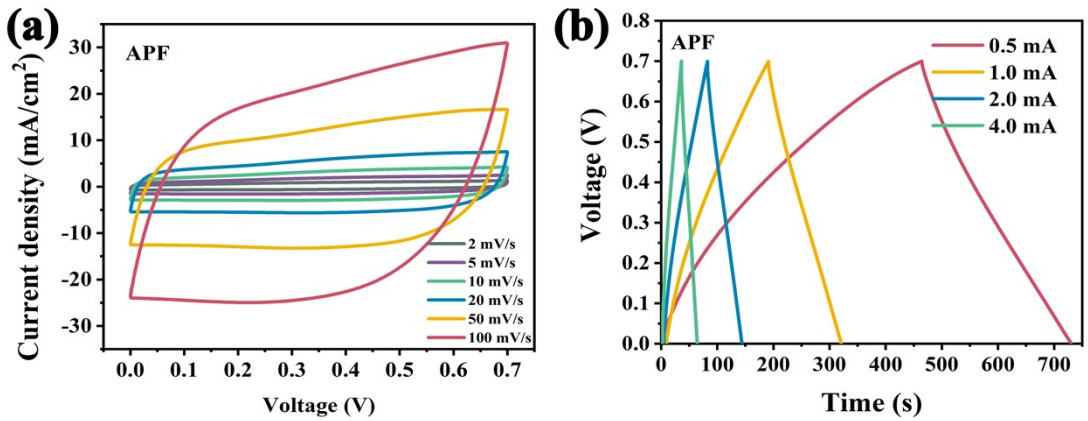

Figure S4 (a) The CV curves of all-solid-state supercapacitors based on $BMIMBF_4$ gel electrolyte at various scan rates and (b) the GCD curves at different discharge currents with APF as electrodes.

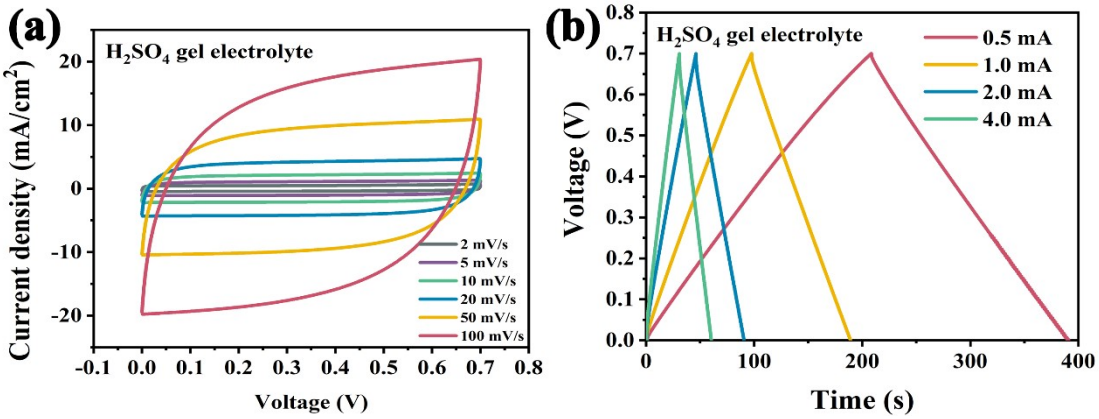

Figure S5 (a) The CV curves of all-solid-state supercapacitors based on H_2SO_4 gel electrolyte at various scan rates and (b) the GCD curves at different discharge currents with APGF as electrodes.

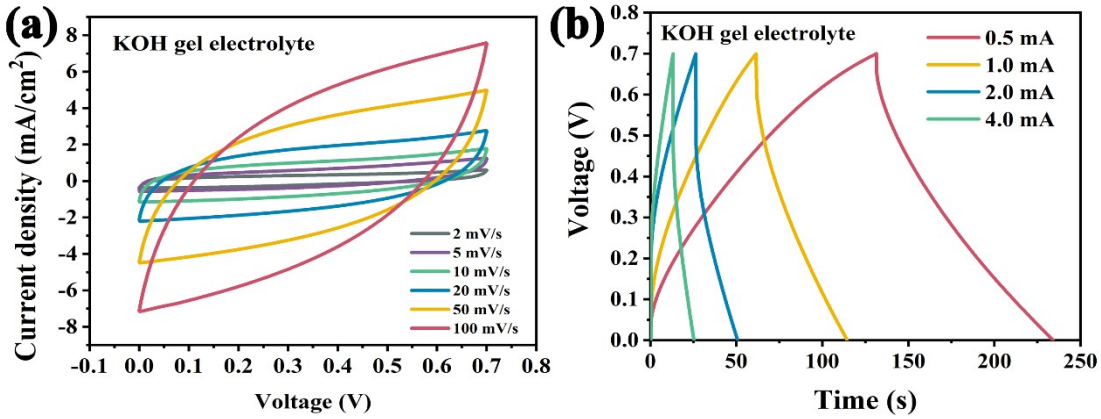

Figure S6 (a) The CV curves of all-solid-state supercapacitors based on KOH gel electrolyte at various scan rates and (b) the GCD curves at different discharge currents with APGF as electrode.

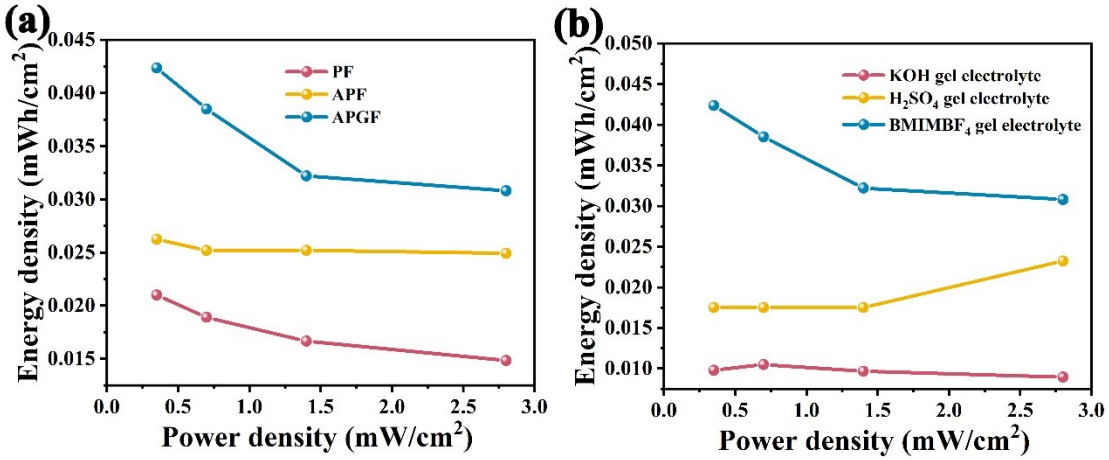

Figure S7 The Ragone plots of all-solid-state supercapacitors based on (a) different electrodes and (b) different gel electrolytes.

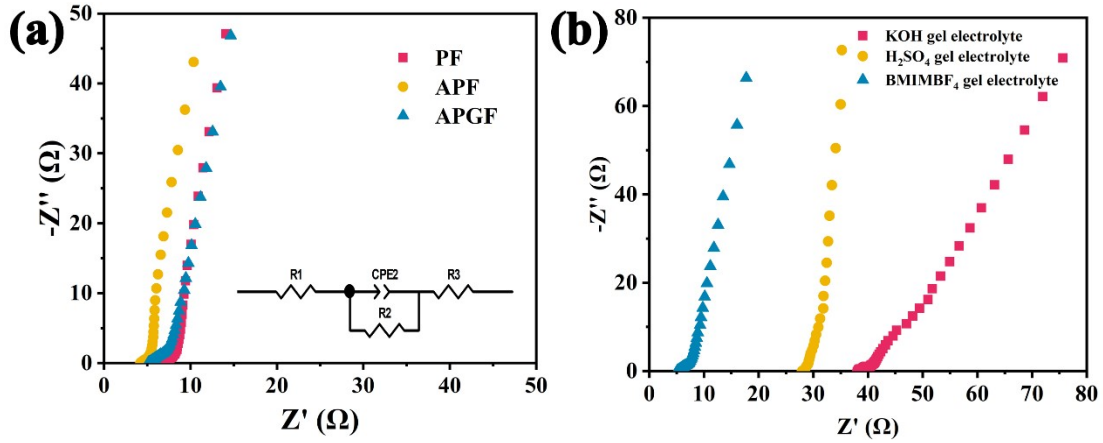

Figure S8 The Nyquist plots spectra of all-solid-state supercapacitors based on (a) different electrodes and (b) different gel electrolytes. The inset of (a) is the equivalent series circuits of the Nyquist plots.

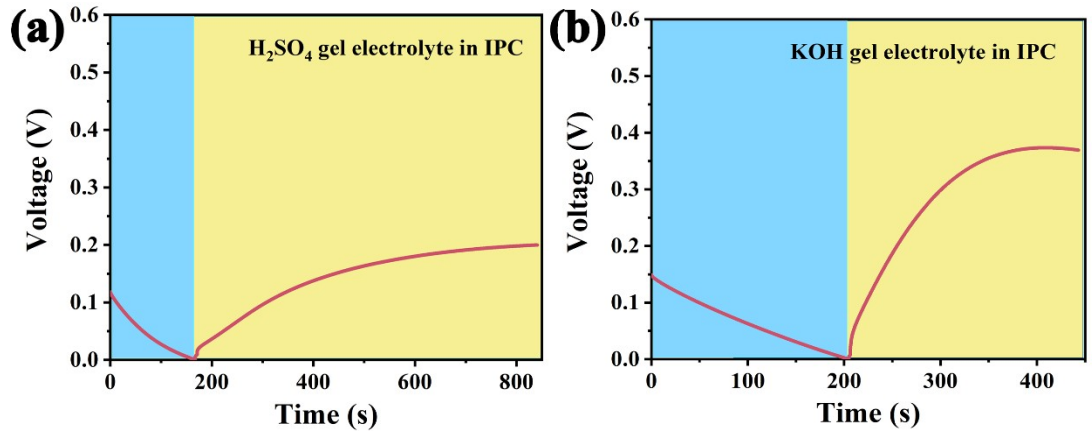

Figure S9 Photo-charge/ galvanostatic-discharge performance of IPC based on (a) H_2SO_4 gel electrolyte and (b) KOH gel electrolyte.

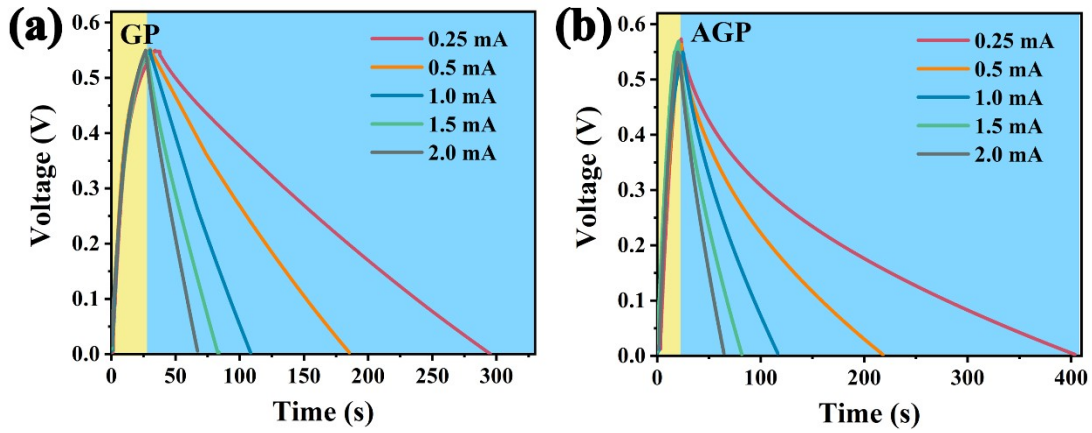

Figure S10 Photo-charge/ galvanostatic-discharge performance of IPC based on GP and AGP electrodes at various discharge currents.

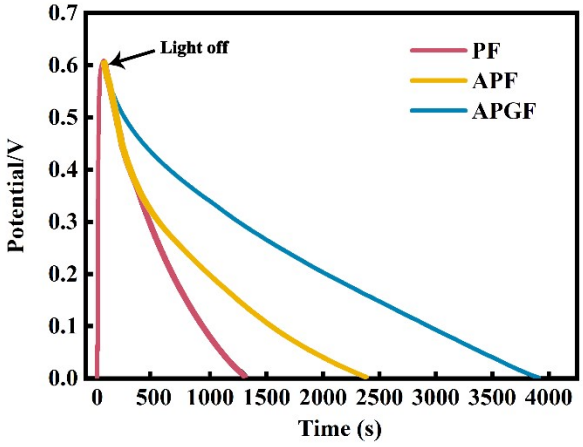

Figure S11 The photo-charging and self-discharging of IPC with various compatible electrodes.

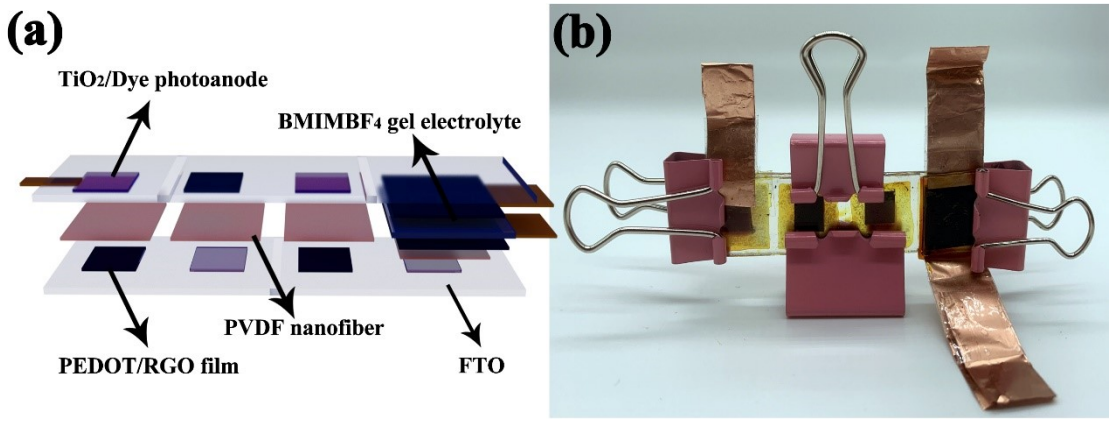

Figure S12 (a) Structure diagram and (b) device diagram of high-voltage IPC.

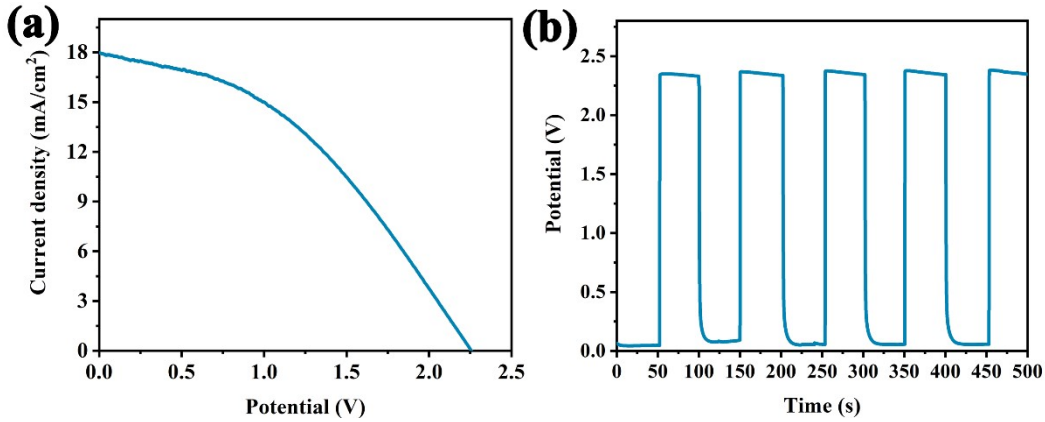

Figure S13 (a) The J-V curve and (b) the open circuit voltage of series photoanode modules.

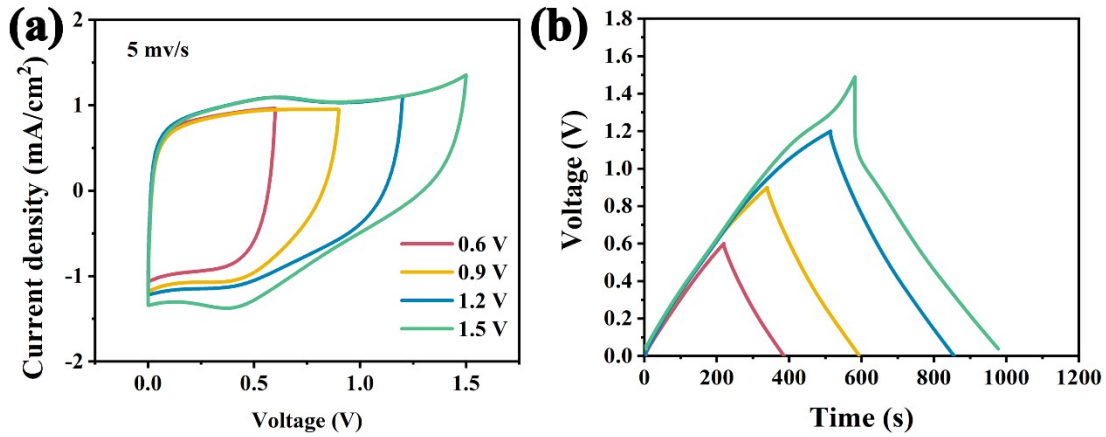

Figure S14 (a) The CV curves and (b) the GCD curves of all-solid-state supercapacitors based on $BMIMBF_4$ gel electrolyte and APGF as electrodes at various voltage windows.

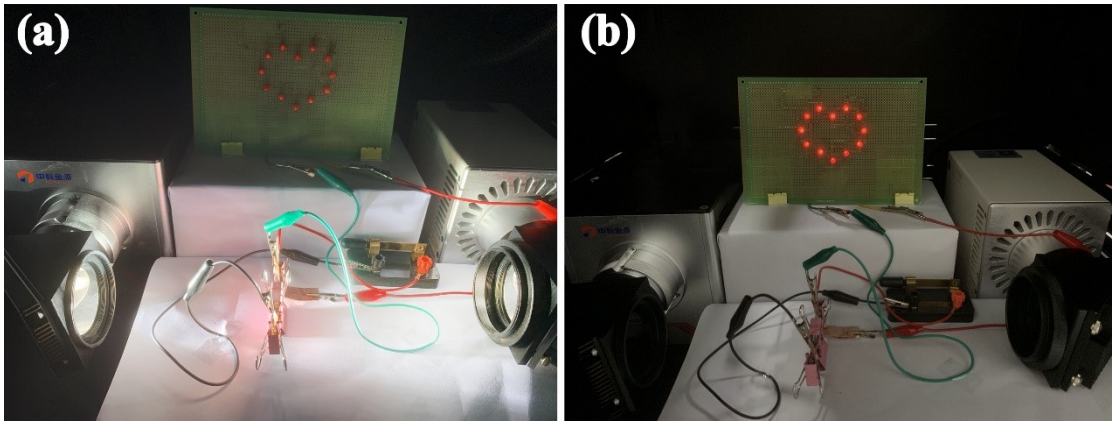

Figure S15 The photography of LEDs lightened by high-voltage IPC (a) under illumination and (b) under dark.

Table S1 Performance of IPCs based on various compatible electrodes

Flexible/ Rigid	Compatible Electrode	Specific Capacitance	Photoconversion Efficiency	Overall Efficiency	Ref.
Rigid	PANI/CNT paper	422 mF/cm^2	22.1%	0.77%	[1]
Rigid	bi-polar TiO_2 nanotube	1.1 mF/cm^2	3.17%	1.64%	[2]
Rigid	PEDOT film	30 mF/cm^2	3.84%	2%	[3]
Rigid/ Flexible	FTO glass / ITO-PEN	21.25 F 17.27 F	14.14% 10.80%	2.13% 1.27%	[4]
Rigid	FTO glass	183 F/g	6.11%	/	[5]
Rigid	$NiCo_2O_4$@ carbon paper	400F/g	13.79%	4.08%	[6]
Flexible	CF@TiO_2@ MoS_2	18.51 mF/cm^2	9.5%	1.8%	[7]
Flexible	Ti_3C_2Tx film	502 mF/cm^2	13.6%	2.2%	[8]
Flexible	Carbon nanotube yarn	78.26 mF/cm^2	5.5%	4.69%	[9]
Flexible	PEDOT: PSS/Ag fiber	52 mF/cm^2	6.43%	4.94%	[10]
Flexible	bi-polar TiO_2 nanotube	262.5 mF/cm^2	5.6%	4.9%	[11]
Flexible	PEDOT fiber	251.2 mF/cm^2	7.3%	5.1%	[12]
Rigid/ Flexible	PEDOT/RGO film	418.57 mF/cm^2	6.87%	5.8%	This work

Reference

1 R. Liu, C. Liu, S. Fan, *J. Mater. Chem. A,* 2017, **5,** 23078.

2 J. Xu, H. Wu, L. Lu, S.-F. Leung, D. Chen, X. Chen, Z. Fan, G. Shen, D. Li, *Adv. Funct. Mater.,* 2014, **24,** 1840.

3 Y. Jin, Z. Li, L. Qin, X. Liu, L. Mao, Y. Wang, F. Qin, Y. Liu, Y. Zhou, F. Zhang,

Adv. Mater. Inter., 2017, ***4*****,** 1700704.

4 Y. Yang, L. Fan, N.D. Pham, D. Yao, T. Wang, Z. Wang, H. Wang, *J. Power Sources,* 2020, **479,** 229064.

5 A. Das, S. Deshagani, R. Kumar, M. Deepa, *ACS Appl. Mater. Inter.,* 2018, **10,** 35932.

6 P. Chen, T.-T. Li, G.-R. Li, X.-P. Gao, *Sci.China Mater.,* 2020, **63,** 1693-1702.

7 J. Liang, G. Zhu, C. Wang, Y. Wang, H. Zhu, Y. Hu, H. Lv, R. Chen, L. Ma, T. Chen, Z. Jin, J. Liu, *Adv. Energy Mater.,* 2017, **7,** 1601208.

8 L. Qin, J. Jiang, Q. Tao, C. Wang, I. Persson, M. Fahlman, P.O.Å. Persson, L. Hou, J. Rosen, F. Zhang, *J. Mater. Chem.* A, 2020, ***8*****,** 5467.

9 J.H. Kim, S.-J. Koo, J.Y. Cheon, Y. Jung, S. Cho, D. Lee, J.W. Choi, T. Kim, M. Song, *Nano Energy,* 2022, **96,** 107054.

10 W.Y. Jin, M.M. Ovhal, H.B. Lee, B. Tyagi, J.W. Kang, Scalable, *Adv. Energy Mater.,* 2020, **11,** 2003509.

11 F. Zhang, W. Li, Z. Xu, M. Ye, H. Xu, W. Guo, X. Liu, *Nano Energy,* 2018, **46,** 168.

12 Z. Wang, J. Cheng, H. Huang, B. Wang, *Energy Stor. Mater.,* 2020, **24,** 255.